Magnetism and magnetization dynamics in thin film ferromagnets

Verhagen, T.G.A.

Citation

Verhagen, T. G. A. (2014, February 26). *Magnetism and magnetization dynamics in thin film ferromagnets*. *Casimir PhD Series*. Retrieved from https://hdl.handle.net/1887/24306

Author: Verhagen, T.G.A.
Title: Magnetism and magnetization dynamics in thin film ferromagnets
Issue Date: 2014-02-26

APPENDIX A

Hall measurements

The presence of a spin-orbit torque (SOT) can also be investigated using Hall measurements. In Figure A.1 a schematic diagram is shown to measure the Hall voltages. When current flows through the device under test, the current can induce an effective field $\Delta\mathbf{H}$, which consists of the Oersted field, the STT-field and the SOT-fields. This effective field can modify the polar angle θ_M and azimuthal angle ϕ_M of the magnetization direction from the equilibrium value (θ_{M0}, ϕ_{M0}) by a small angle ($\Delta\theta_M$ and $\Delta\phi_M \ll 1$), where $\Delta\theta_M$ and $\Delta\phi_M$ are the change in the polar and azimuthal magnetization angle. They are then equal to

$$\theta_M = \theta_{M0} + \Delta\theta_M, \tag{A.1}$$

$$\phi_M = \phi_{M0} + \Delta\phi_M, \tag{A.2}$$

where $\Delta\theta_M$ and $\Delta\phi_M$ can be derived from the total free energy F per unit volume of magnetization of the film (equation 5.3) [174].

The Hall voltage V_H in a ferromagnet contains a contribution of the anomalous Hall effect (AHE) and the planar Hall effect (PHE) [175]

$$V_H = I\left[R_{\text{AHE}}\cos\theta_M + R_{\text{PHE}}\sin^2\theta_M\sin 2\phi_M\right], \tag{A.3}$$

where R_{AHE} and R_{PHE} are the contributions in the Hall resistance due to the AHE and PHE, and I is the bias current. An oscillating current $I_{\text{ac}}\sin\omega t$ is used to induce an effective field modulation $\Delta\mathbf{H}\sin\omega t$ that can modify the magnetization direction. When equations A.1 and A.2

are substituted in equation A.3, the Hall voltage is equal to [174]

$$V_{XX}(\theta_H, \phi_H) = V_0(\theta_H, \phi_H) + V_\omega(\theta_H, \phi_H)\sin\omega t + V_{2\omega}(\theta_H, \phi_H)\cos 2\omega t, \tag{A.4}$$

where the coefficients $V_0(\theta_H, \phi_H)$, $V_\omega(\theta_H, \phi_H)$ and $V_{2\omega}(\theta_H, \phi_H)$ depend on the system studied [174].

The first harmonic term V_ω relates to the equilibrium direction of the magnetization and is independent of the modulated fields. The second harmonic term $V_{2\omega}$ measures the change from the equilibrium direction of the magnetization due to the current-induced fields. By studying the angular dependence of the harmonic terms, the symmetry of the SOI can be derived from which the physical mechanism can be reconstructed. Note that, in equation A.3, the first harmonic term is in-phase with the driving current, while the second harmonic term is out-of-phase. The measurements were performed by using two lock-in detectors for the longitudinal and transverse voltages, respectively.

Figures A.2 and A.3 show our first measurements of the Hall coefficients for the SiO_x/Co(2.6)/Cu bilayer and Cu/Co(2.6)/Cu trilayer as a function of the applied magnetic field. The current density used to measure the Hall voltages is different for both samples. For the SiO_x/Co/Cu, a much larger current density was needed to have a reasonable signal-noise ratio.

A clear difference between both samples is visible. The in-phase first harmonic term of the Cu/Co(2.6)/Cu trilayer shows parabolic behaviour (Figure A.3.a and c) and when the first harmonic term is split

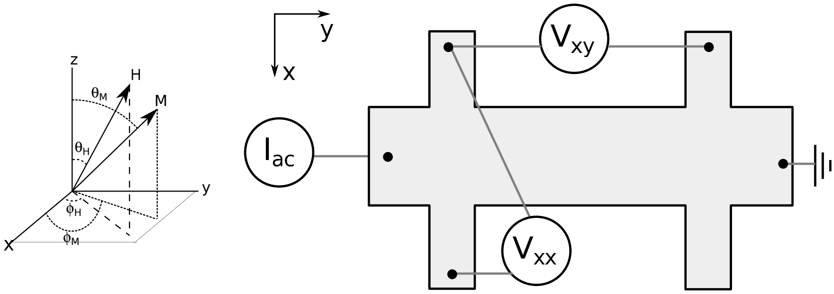

Figure A.1: Coordinate system used for the Hall measurements. A current I_{ac} is applied along the y-direction and a magnetic field is applied along the x-direction ($\theta_M = 90°$, $\phi_M = 0°$), and the Hall voltage V_{xx} is measured along the x-direction.

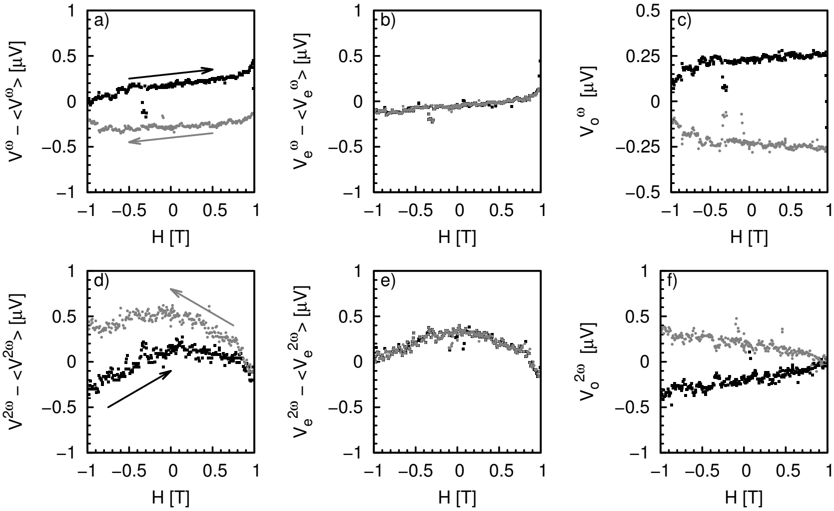

Figure A.2: Hall measurements on the SiO_x/Co(2.6)/Cu bilayer with I_{ac} = 40 mA (current density is $6 \cdot 10^{10}$ A/m^2). The in-phase first harmonic term V^{ω} is shown in a), where b) is the even part V_e^{ω} and d) the odd part V_o^{ω} of the first harmonic term respectively. d–f) show the out-of-phase component of the second harmonic term $V^{2\omega}$, which can also be split in an even and odd part. The arrows indicate the direction of the magnetic field sweep. For clarity, a constant offset $< V >$ is subtracted from the harmonic terms.

into even and odd parts, the even term shows also a parabola while the odd term is virtually absent. The SiO_x/Co/Cu bilayer shows different behaviour for the first harmonic term. First, there is a large offset present, which is removed in Figure A.2. Secondly, no parabola is visible, but the first harmonic term is linear and there is an offset between the measured voltage for the up and down magnetic sweep. Furthermore, at -1 T the measured voltage of the up and down sweep bend to each other which is clearly visible in Figures A.2.c, whereas at +1 T both sweeps bent in the same direction.

For both samples the out-of-phase second harmonic term shows behaviour very similar to the first harmonic term. The Cu/Co/Cu trilayer again shows a parabola. The SiO_x/Co/Cu bilayer again shows linear behaviour, but there is now a clear bend visible around 0 T as is shown in Figures A.2.d. When the second harmonic term is split into an odd and even part, the even part now also looks like a parabola (see Fig-

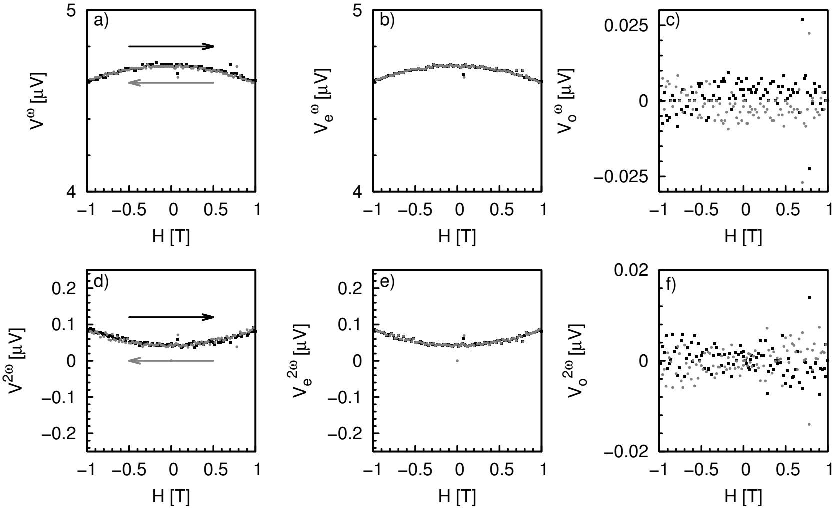

Figure A.3: Hall measurements on the Cu/Co(2.6)/Cu trilayer with I_{ac} = 1 mA (current density $9 \cdot 10^8$ A/m^2). The in-phase first harmonic term V_x^{ω} is shown in a), where b) is the even part V_e^{ω} and c) the odd part V_o^{ω} of the first harmonic term respectively. d–f) show the out-of-phase component of the second harmonic term $V^{2\omega}$, which can also be split in an even and odd part. The arrows indicate the direction of the magnetic field sweep.

ure A.2.e) and the odd part is linear while both branches appear to cross each other at approximately +1 T (see Figures A.2.f), which happens to be the maximum field of the sweep.

A.1 Discussion

Summarizing the provisional experimental findings, the Hall measurements of a SiO$_x$/Co(2.6)/Cu bilayer and a Cu/Co(2.6)/Cu trilayer show very different behaviour. The spin Hall angle of Cu is very small, so no influence of the SHE and Rashba effect is expected for the Cu/Co(2.6)/Cu trilayer. This was already confirmed in Chapter 6 using FMR measurements on Cu/Co/Cu trilayers. However, in the SiO$_x$/Co(2.6)/Cu bilayer, broken inversion symmetry is present which resulted in an unexpected large damping in FMR measurements.

In Figure A.3.a the in-phase first harmonic coefficient of the Cu/Co(2.6)/Cu trilayer shows parabolic behaviour. The first harmonic coefficient is due to the equilibrium magnetization. Figures A.3.b and c show that the measured in-phase first harmonic coefficient consist mostly of an even, planar Hall, term. In contrast the in-phase first harmonic coefficient of the $\mathrm{SiO_x}$/Co(2.6)/Cu bilayer now consists now of an even, planar Hall, term and an odd, anomalous Hall, term. We do not yet fully understand the behaviour of this bilayer with a built-in lack of inversion symmetry and although both samples were glued on the same sample holder, a small misalignment could be present.

Pi et al. [176] measured the in-phase first and out-of-phase second harmonic coefficients of a Ta(5)/Pt(3)/Co(0.6)/$\mathrm{AlO_x}$(1.8) and a Ta(5)/Pt(3)/Co(0.6)/Pt(3) multilayer and they noticed a clear difference between the symmetric Pt/Co/Pt trilayer and asymmetric Pt/Co/$\mathrm{AlO_x}$ trilayer. Whereas the out-of-phase second harmonic coefficient of the asymmetric trilayer shows a parabolic shape, the measured out-of-phase second harmonic coefficient of the symmetric trilayer shows a negligible signal. They contribute the difference between the symmetric and asymmetric trilayer to the presence of a Rashba field in the asymmetric trilayer.

Hall measurements done on other metallic asymmetric multilayers [59, 169, 176, 177] suggest that beside the Rashba SOT also a spin Hall SOT exists. Kim et al. [59] showed for a Si/Ta(d)/CoFeB(1)/MgO(2)/Ta(1) multilayer that the odd part of the second harmonic coefficient consists of two linear signals, lines, where each line corresponds to an initial perpendicular magnetization orientation, that cross each other at a certain field. For a Ta bottom layer of 1 nm, the lines cross each other at zero field. When decreasing the thickness of the Ta bottom layer to 0.1 nm, they observe that both lines cross each other now at -0.1 T. They attribute this change in crossing field to a change from the spin Hall SOT for larger Ta thicknesses to the Rashba SOT for very small Ta thicknesses. In our $\mathrm{SiO_x}$/Co(2.6)/Cu multilayer, we observe that the lines cross at a finite field although we did not create a well-defined initial magnetization orientation. The non-zero crossing suggests that a Rashba SOT is present in our $\mathrm{SiO_x}$/Co(2.6)/Cu bilayer. However, the crossing of the up- and down-sweep happens around the maximum field of our magnet (+1 T) so that a full crossing cannot be observed, and the hysteresis present in the second harmonic shows similarity with the hysteresis present in the first harmonic coefficient.

The presence of a second harmonic coefficient indicates that there is a current induced field present. Beside the SOT, the applied current can also produce an Oersted field and heating. Ohmic heating is independent of external field and current directions and increases the temperature of the sample. The increase in temperature decreases the magnetic anisotropy field and the saturation magnetization of the magnetic layer. Garello et al. [169] showed that heating effects are most clearly visible in the third harmonic coefficient, which is not measured in our experiment. Heating also appears as a contribution to the second harmonic coefficient, but heating effects have only a minor influence on the spin torque measurements [169]. The resistance of the 50 $\times 1000$ μm^2 Cu/Co(2.6)/Cu Hallbar is approximately 90 Ω, so current of 1 mA generates approximately 0.1 mW of heat, well below the 40 mW that was dissipated in a 10 $\times 60$ μm^2 Ta(1)/CoFeB(1)/MgO(2)/Ta(1) Hallbar used in the experiments of Kim et al. [59], that gave rise to a temperature increase of the wire of approximately 10 K. For the Cu/Co/Cu and SiO_x/Co/Cu multilayers, the Oersted fields are approximately 0.1 G and 5 G respectively, smaller than the values of the SOT fields from the FMR data and other experiments [59, 169]. So we expect that the influence of the current induced heating and Oersted field are small.

Ryu et al. [178] and Emori et al. [177] showed that domain walls in Ta(3)/Pt(3)/CoFeB(0.6)/MgO(1.8)/Ta(2), Ta(5)/CoFeB(0.6)/MgO(1.8)/Ta(2) and TaN(2)/Pt(1.5)/Co(0.3)/Ni(0.7)/Co(0.15)/TaN(5) multilayers flow against the electron flow. Although the multilayers are asymmetric and contain heavy metals, the direction of the induced Rashba and spin Hall torque cannot explain the movement of the domain walls against the electron flow. The Dzyaloshinskii-Moriya interaction (DMI) needs to be taken into account to explain this observation. Moon et al. [179] and Cortés-Ortuño and Landeros [180] calculated how the DMI would change the spin-wave dispersion. An et al. [181] measured using the Brillouin light scattering technique the spin wave spectrum of a CoFeB/Ta bilayer and showed that the spin wave amplitude can be attenuated or amplified depending on the direction of the applied current and magnetic field. Still, with FMR only the $k = 0$ wavevector is probed and the DMI should not have effect on the measured FMR spectrum. Nonetheless, the DMI can play an important role in the Hall measurements. It does not explain the huge increase in ΔH_{pp} in the FMR spectra of the SiO_x/Co(d)/Cu and SiO_x/Co(2.6)/Pt multilayers.

To conclude, we tentatively attribute the observed odd out-of-phase second harmonic coefficient in the SiO_x/Co(2.6)/Cu bilayer to the Rashba SOT.